2023 Volume 1, Issue 2
Computer Simulation in Application
ISSN: 2630-4597 (Online)

Exploration of the Heat Treatment Process of Wind Turbine Main Shafts Based on Computer Simulation Technology

Xin Xie[1]*, Feng Gu[2], Yuan You[2], Yifan Wang[2], Wenping Sheng[2], Yan Wang[2], Jie Wu[2]
[1]Network Information Center, Qiqihar University, Qiqihar 161006, Heilongjiang Province, China
[2]School of Materials Science and Engineering, Key Laboratory of Polymer Matrix Composites in Heilongjiang Province, Qiqihar University, Qiqihar 161006, Heilongjiang Province, China

Corresponding author: Xin Xie, 4086645@qq.com

Abstract:

Based on computer simulation technology, the finite element simulation of the heat treatment process for 42CrMo4 alloy steel wind turbine main shafts was conducted. Changes in the temperature field, stress field, phase field, and hardness field during the heat treatment process were analyzed. Simulation results indicated that the water quenching process generated significant stress, with a maximum stress of 354 MPa. However, tempering could reduce the stress caused by water quenching, with the corresponding maximum stress decreasing to 119 MPa. After water quenching, the main shaft obtained a martensite volume fraction of approximately 10%, achieving a maximum hardness of 50.9 HRC. The increase in hardness was directly proportional to the martensite content. Following high-temperature tempering, martensite could be transformed into tempered sorbite, resulting in a hardness reduction to 30 HRC. The final microstructure of the main shaft after heat treatment consisted of pearlite, bainite, tempered sorbite, and ferrite, with a hardness range of 26.8 to 30 HRC. This demonstrates that computer simulation technology can predict the heat treatment results of large forgings, providing a theoretical basis for developing heat treatment processes.

Keywords:

Computer simulation
Main shaft
Heat treatment
Finite element

Online publication: December 22, 2023

1. Introduction

In recent years, with the increasing emphasis on environmental protection, the demand for clean energy has been growing steadily, leading to rapid development in wind power generation [1]. As a core component of wind turbines, the wind turbine main shaft connects to the generator through a rubber coupling after passing through the bearing and increasing speed in the gearbox [2]. It plays a crucial role in transmitting torque and requires highly comprehensive mechanical properties. 42CrMo4 alloy steel, with its excellent mechanical properties, is the primary steel used for wind turbine main shafts [3]. Quenching and tempering, the most commonly used heat treatment process, involves quenching the workpiece followed by high-temperature tempering. This process improves the workpiece's comprehensive mechanical properties without changing its composition. Many scholars have studied the quenching and tempering process of 42CrMo4 alloy steel, focusing on quenching process design [4], quenching medium selection [5], and tempering temperature choice [6]. By arranging the cooling sequence of quenching media, preparing cooling media with higher heat transfer coefficients, and optimizing the tempering temperature, the quenching and tempering process can be optimized to achieve better mechanical properties. Computer simulation technology is now widely used in industrial production, helping enterprises improve efficiency and reduce trial-and-error costs during production process development. Many scholars have conducted research on computer simulation technology for heat treatment, using the finite element method to simulate the quenching and carburizing processes of small parts such as gears, pistons, and samples. These simulations analyze the heat treatment process from both thermal and mechanical perspectives [7-11]. However, computer simulation of the heat treatment process for large forgings like wind turbine main shafts is relatively rare. In this paper, computer simulation technology is used to model 42CrMo4 alloy steel wind turbine main shafts, establish a material database, and perform finite element simulation of the heat treatment process. Changes in the temperature field, stress field, phase field, and hardness field during the heat treatment of the main shaft are analyzed and compared with experimental results from published papers, providing theoretical support for the development of heat treatment processes for wind turbine main shafts.

2. Simulation process

2.1. Model establishment

In this paper, the main shaft component from a 4 MW wind turbine is adopted [6], and the material used is 42CrMo4. The specific chemical composition is shown in **Table 1**. The UG software is utilized to create a three-dimensional model of the main shaft. The maximum dimension in the length direction of the main shaft is 3,110 mm, and the maximum radial dimension is at the flange with a diameter of 1,870 mm. The core of the main shaft has a hollow structure with a through-hole diameter of 380 mm.

2.2. Material database establishment

The JMATPRO calculation software is employed to compute the mechanical, thermal, and phase transformation properties of 42CrMo4 alloy steel. By entering the chemical composition of 42CrMo4 into the software, the phase transformation curve of the material from 20 to 1,600°C is calculated, as shown in **Figure 1(a)**. Due to the addition of alloy elements, the austenite-ferrite transformation temperature of 42CrMo4 alloy steel changes compared to the phase transformation curve of ordinary carbon steel. Through software calculation, the austenite-ferrite transformation temperature range is determined to be 718.3 to 770.9°C. To ensure complete austenitization, the heat treatment quenching heating temperature is typically set 50 to 70°C higher than this temperature range.

Table 1. Chemical composition of 42CrMo4 [mass fraction (%)]

Elements	C	Mn	Cr	Mo	Si	P	S	Fe
Composition control	0.38~0.45	0.60~0.90	0.90~1.20	0.15~0.30	≤ 0.40	≤ 0.035	≤ 0.035	Bal.
Actual values	0.39	0.64	1.08	0.16	0.21	0.007	0.002	Bal.

The calculation of the hardenability curve for 42CrMo4 material is equally important because quenching is the most crucial part of heat treatment, and the hardenability curve is the primary parameter reflecting the quenching characteristics of the material. By setting the grain size of the component to 7.5 [6], the quenching heating temperature to 840℃, and selecting a hardenability sample length of 20 cm, recording every 0.5 cm, we can obtain the hardenability curve as shown in **Figure 1(b)**. The data from this curve can be used in subsequent heat treatment simulations. Due to the significant temperature difference between the component surface and the cooling medium, the cooling rate is fast, resulting in a dense microstructure and smaller grains. Therefore, the surface hardness and strength are relatively high. As the distance from the surface increases, both strength and hardness decrease significantly.

Using the DEFORM-HT material data generation function in JMATPRO, a .key file that can be directly used in finite element software is generated. This file includes the elastoplastic and thermodynamic properties of the material. During the calculation, it is essential to use 840℃ as the heat treatment temperature (70℃ higher than the calculated austenite-ferrite transformation temperature). The generated file contains the CCT curve, as shown in **Figure 1(c)**, which can be incorporated as basic data into the finite element simulation.

2.3. Finite element simulation

The heat treatment process of the 42CrMo4 alloy steel wind turbine main shaft is simulated using DEFORM-HT software. The specific simulation process is shown in **Figure 2(a)**. The finite element simulation is mainly divided into three parts: pre-processing, finite element simulation, and post-processing. Pre-processing mainly involves loading the model, meshing, and setting initial boundary conditions and process parameters. Finite element simulation automatically calculates the pre-processed data using numerical iteration methods. Post-processing allows for the analysis of simulation results using analytical tools.

During pre-processing, the established model and database need to be imported. It is important to note that due to the high symmetry of the DEFORM-HT heat treatment simulation, to save time and reduce computational steps, only 1/18 of the wind turbine main shaft can be selected for simulation, as highlighted in **Figure 2(b)**. After the simulation is complete, the post-processing mirroring tool can be used to restore the entire main shaft. Since the phase transformation data in the .key file generated by JMATPRO is not sufficient, the simulation needs to use the phase transformation data from the Demo temper steel material module provided by DEFORM-HT. This module includes parameters for the mutual transformation of eight common phases in steel, enabling a more accurate representation of phase field changes during heat treatment. The elastoplastic and thermodynamic data of 42CrMo4 from the .key file generated by JMATPRO replaces the corresponding data in Demo temper steel, and the hardenability curve data of 42CrMo4 is also input into the Demo temper steel module.

Meshing is crucial for finite element simulation. For larger parts, the mesh needs to be finer to prevent simulation errors. Therefore, the mesh of this wind turbine main shaft is divided into 20,000 tetrahedrons [3], as shown in **Figure**

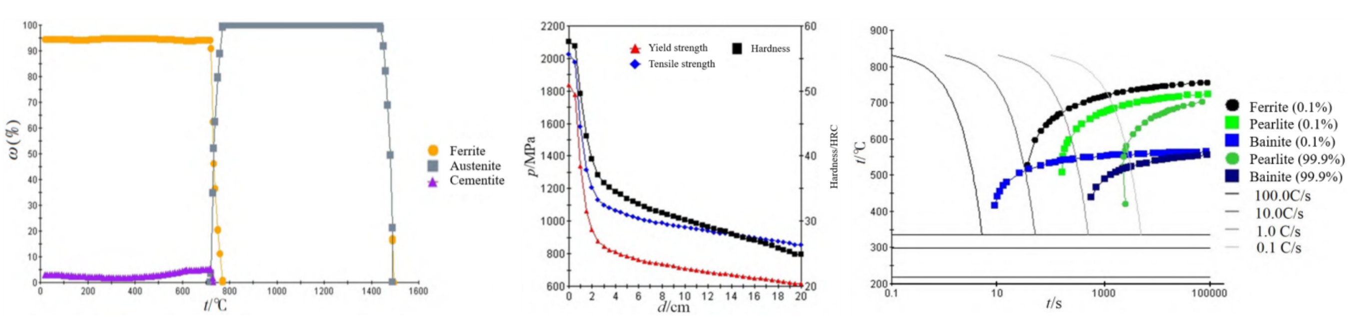

(a) Austenite-Ferrite transformation curve with temperature for 42CrMo4 alloy steel (b) Hardenability curve of 42CrMo4 alloy steel (c) CCT curve of 42CrMo4 alloy steel

Figure 1. Basic data curves for heat treatment of 42CrMo4 material

2(c). Tetrahedral meshes, which are more adaptable to complex geometric shapes, are used for this finite element simulation to facilitate free mesh generation. Since the simulated part is relatively large, the influence of tetrahedral and hexahedral meshes on the stress field can be neglected. During the initial condition setup, two large planes in the main shaft are set as symmetrical planes, and the cusp at the small diameter end is set as the boundary. The initial carbon concentration is set to 0.39%. As the main shaft undergoes normalization as a preparatory heat treatment before the final heat treatment, the initial phase composition is set to the normalized structure of pearlite and bainite.

The heat treatment process and medium parameters are set, and the specific process is presented in **Table 2**. The quenching heating temperature is set to 840°C, and the heating time is calculated using the heating parameter × equivalent thickness based on empirical formulas. The heating parameter for alloy steel is approximately 1.3 to 1.6 [12,13]. Due to the high quenching heating temperature, the lower limit of 1.3 is chosen; for the lower tempering temperature, the upper limit of 1.6 is selected. The equivalent thickness (maximum thickness) of the model is measured by software to be 160 mm. The simulated wind turbine main shaft has a maximum length of over 3 meters and a weight of 10.4 tons. The heat treatment equipment used is a fuel heat treatment furnace with gas as the main heat source, and the heat transfer method is radiation + convection. However, due to the large size of the heat treatment furnace and high heating temperature, radiation is chosen as the main heat exchange method for this simulation. The heat exchange coefficient for ordinary resistance furnace heating is 0.1 N/s/mm/°C. Determining the heat exchange coefficient for water cooling is crucial. The model is divided into two zones: one is the water direct contact zone (Qwdc), and the other is the water indirect contact zone (Qwic). The heat exchange coefficient for Qwdc is α(t) [3], which varies with temperature as shown in **Table 3**. The heat exchange coefficient for Qwic is 2.2 N/s/mm/°C, and the tempering heat exchange coefficient is 0.4 N/s/mm/°C [12].

Finally, set the temperature change for each step to 2°C, with a minimum simulation time of 0.001 seconds and a maximum time of 10 seconds for each step. Save every 10 steps, verify the data, and generate a DB file to complete the preprocessing. Finite element simulation is

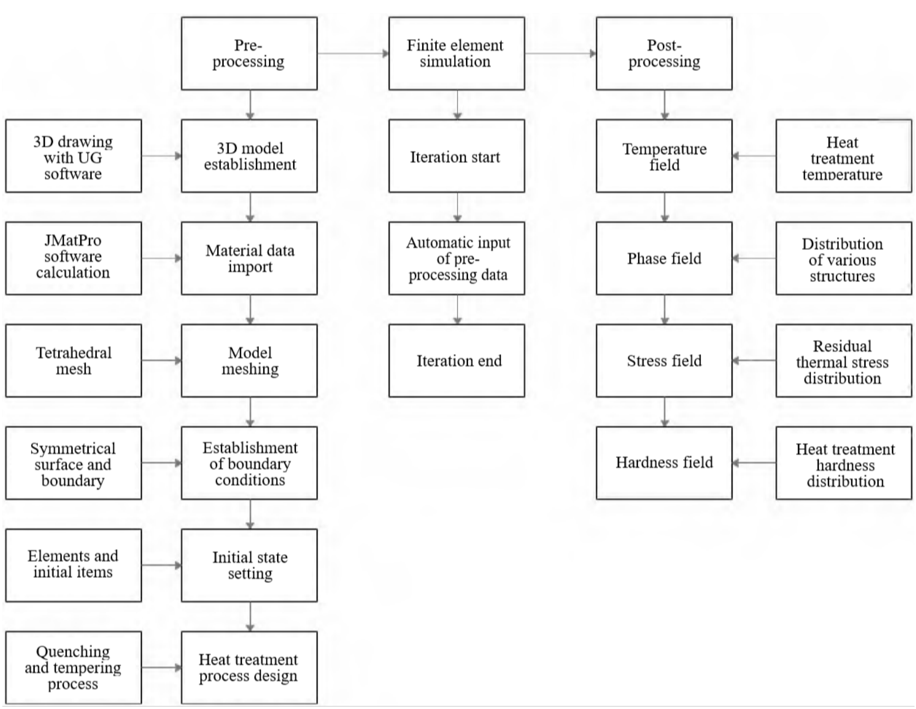

(a) Computer simulation of heat treatment process

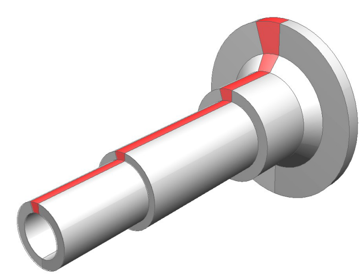

(b) 3D modeling of wind turbine main shaft

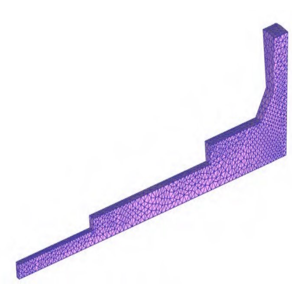

(c) Computer simulation of mesh generation

Figure 2. Computer simulation process and model establishment

Table 2. Heat treatment process parameter settings

Scheduling	*t*/°C	*t*/s	Main heat transfer mode	Heat transfer coefficient / $N \cdot s^{-1} \cdot mm^{-1} \cdot °C^{-1}$
Quenching heating	840	12480	Radiation	0.1
Water cooling	20	3600	Convection	Q wdc, Q wic
Tempering heating	600	15360	Radiation	0.1
Air cooling	20	7200	Convection	0.4

Table 3. Water quenching convective heat transfer coefficient α(t)

t/°C	100	200	300	400	500	600	700	800
$\alpha(t)/N \cdot s^{-1} \cdot mm^{-1} \cdot °C^{-1}$	7.85	27.6	43.56	58.54	74.61	53.62	39.96	4.62

an iterative calculation automatically performed by the computer, and post-processing analysis can be performed after the iteration is complete.

3. Results and discussion

The simulation consisted of a total of 6,980 steps, with quenching heating ending at step 1,560, water quenching ending at step 4,241, tempering ending at step 5,935, and air cooling ending at step 6,980. Post-processing will be carried out in four aspects: temperature field, stress field, phase field, and hardness field. To facilitate viewing the distribution of various fields, the profile of the main shaft is selected for analysis.

3.1. Temperature field

Figure 3 shows the temperature field changes during the heat treatment process. **Figure 3(a)** shows the temperature field distribution during quenching heating. The surface of the main shaft has reached the set temperature of 840°C, while the lowest temperature at the center is 763°C, slightly lower than the ferrite-austenite phase transformation temperature. Theoretically, the quenching heating temperature needs to be further increased to ensure that all parts of the component reach the phase transformation temperature, but an excessively high temperature can lead to coarse grains, resulting in a decrease in overall mechanical properties. As shown in **Figure 3(b)**, the parts directly contacting water are cooled to the same temperature as the water, while the center has not completely cooled, but the difference is not significant. **Figure 3(c)** shows that the tempering temperature is relatively uniform, reaching the preset temperature almost from the inside out, which is related to the lower tempering temperature. Finally, during air cooling (**Figure 3(d)**), like water quenching, the internal temperature is higher. Increasing the cooling time during simulation may improve this situation.

3.2. Stress field

Figure 4 shows the stress field distribution during the heat treatment process. As shown in **Figure 4(a)**, thermal stress is generated during quenching heating, with a maximum of 60.7 MPa, typically occurring at the flange position. This is due to the fact that the flange position in the model has the greatest thickness and requires the most heat for heating, resulting in higher thermal stress. As shown in **Figure 4(b)**, rapid cooling (water quenching) generates significant stress, which is the main cause of cracking in the main shaft. The large variation in diameter size at the flange makes it prone to stress concentration, reaching a maximum of 354 MPa. If this stress exceeds the material's strength limit, cracks will develop in the material. Heat treatment tempering is the best way to remove stress. As can be seen from **Figure 4(c)**, after tempering, the maximum stress of the main shaft has been significantly reduced to 119 MPa, a decrease of 66%. As shown in **Figure 4(d)**, the stress increases somewhat during air cooling, but due to the slower cooling rate, it does not generate excessive stress like water quenching.

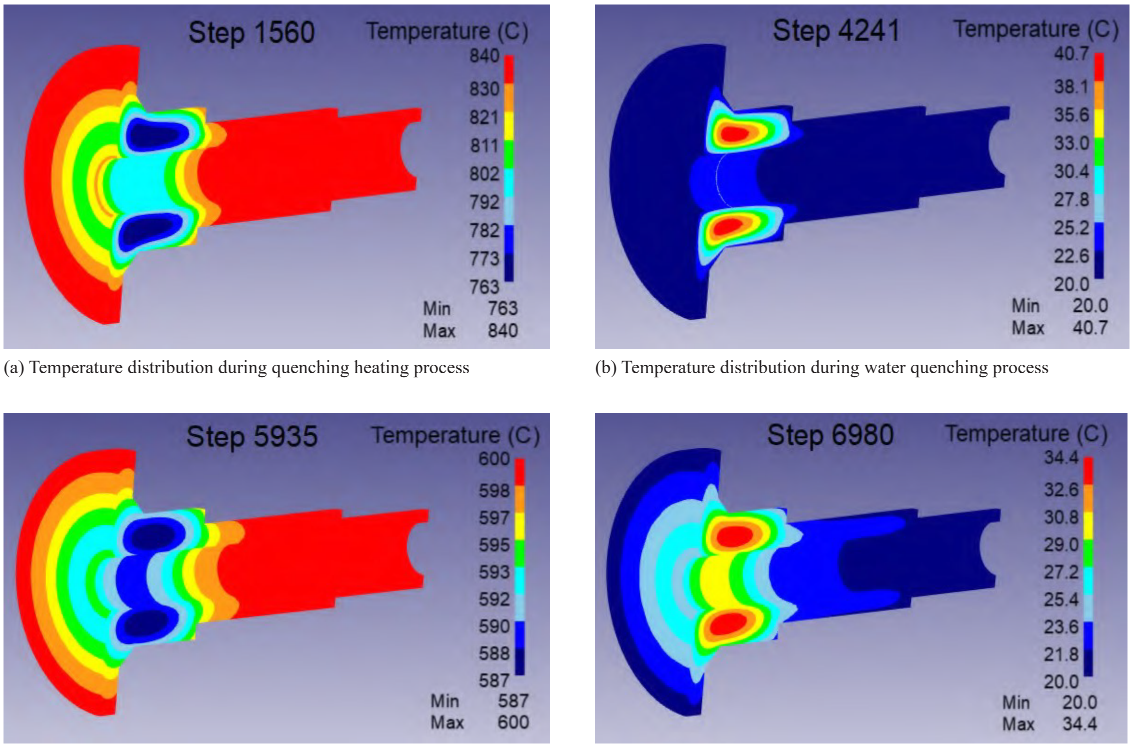

(a) Temperature distribution during quenching heating process

(b) Temperature distribution during water quenching process

(c) Temperature distribution during tempering heating process

(d) Temperature distribution during air cooling process

Figure 3. Temperature field changes during the heat treatment of the fan's main shaft

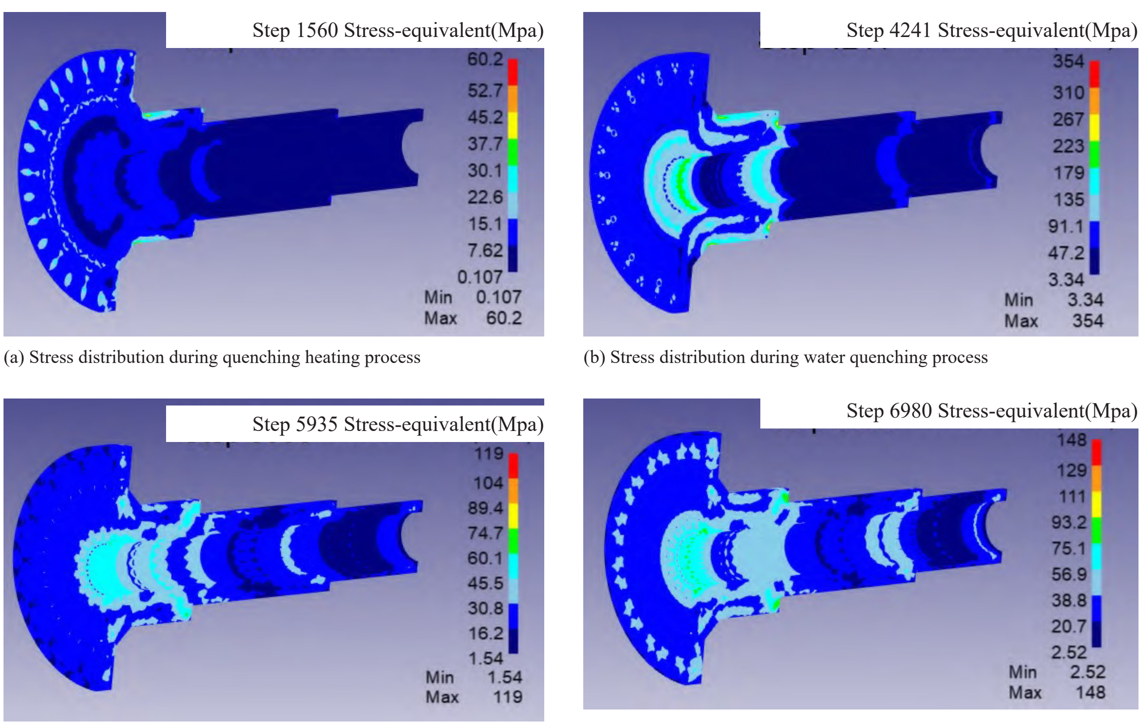

(a) Stress distribution during quenching heating process

(b) Stress distribution during water quenching process

(c) Stress distribution during tempering heating process

(d) Stress distribution during air cooling process

Figure 4. Changes in stress field during heat treatment of the fan's main shaft

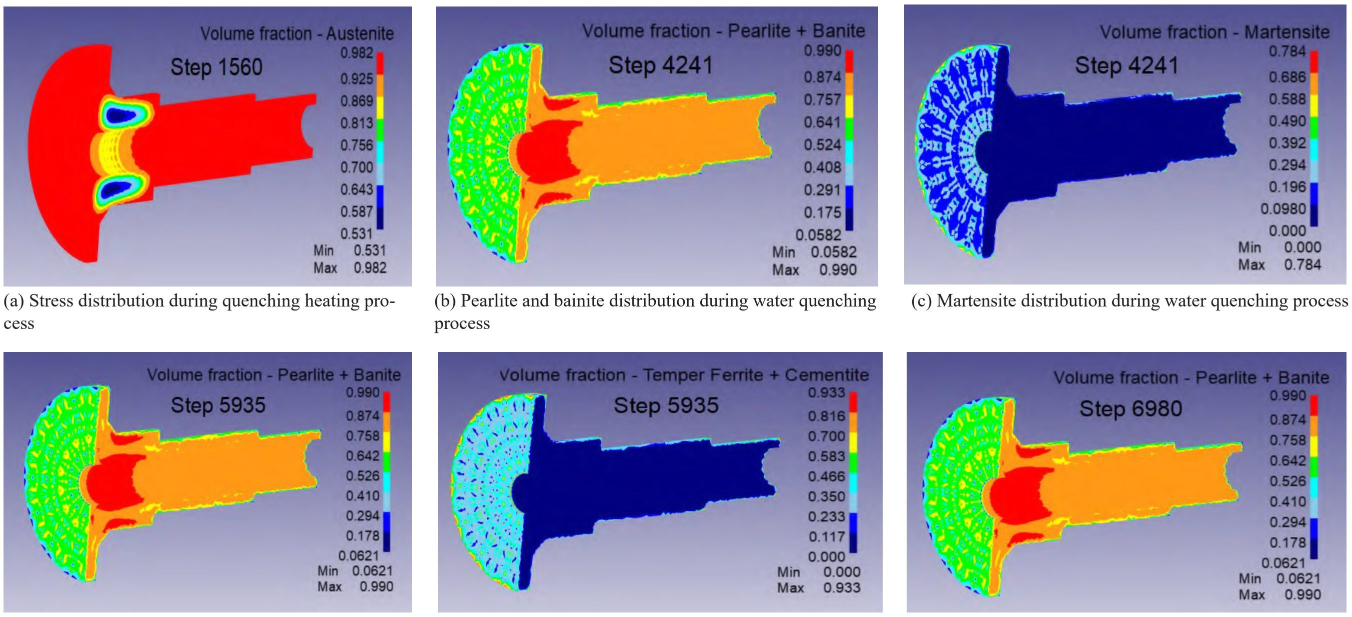

(a) Stress distribution during quenching heating process

(b) Pearlite and bainite distribution during water quenching process

(c) Martensite distribution during water quenching process

(d) Pearlite and bainite distribution during tempering heating process

(e) Tempered sorbite distribution during tempering heating process

(f) Pearlite and bainite distribution during air cooling process

Figure 5. Phase field changes during heat treatment of the fan's main shaft

Maintaining appropriate stress can also lead to strain hardening, increasing the strength of the component, but with a corresponding decrease in ductility

3.3. Phase field

Figure 5 shows the phase field distribution during the heat treatment process. The purpose of quenching heating is to fully austenitize the main shaft. As shown in **Figure 5(a)**, 90% of the main shaft has been austenitized, and only some areas near the core have not transformed into austenite. The austenite distribution is almost consistent with the temperature distribution. Therefore, to achieve complete austenitization, it is necessary to make the core temperature higher than the ferrite-austenite phase transformation temperature. However, excessively high temperatures can also cause coarse grains and reduce mechanical properties. As shown in **Figure 5(b)** and **(c)**, the main phase composition after water quenching is pearlite + bainite + martensite, where martensite is mainly distributed on the surface of the main shaft, and pearlite and bainite are distributed in the core. This mainly depends on the cooling rate. Only a sufficiently fast cooling rate can generate martensite. The surface directly contacts water, resulting in a large heat transfer coefficient and fast cooling rate, thus generating a large amount of martensite. However, because the main shaft is a large, thick-walled component, most areas of the component are distributed with pearlite and bainite. During the tempering stage, as shown in **Figure 5(d)** and **(e)**, the martensite formed by quenching is transformed into tempered sorbite through tempering. Therefore, it can be seen that the distribution of martensite is almost the same as that of tempered sorbite, while pearlite and bainite remain unchanged. During the air cooling stage shown in **Figure 5(f)**, the main structure should be pearlite, with some bainite formation. When using JMATPRO for CCT curve calculation, there are curves for bainite formation and termination. The phase transformation database used in finite element simulation also considers pearlite and bainite together for phase transformation. At this stage, the distribution of pearlite, bainite, and tempered sorbite remains unchanged, indicating that no phase transformation occurs at this point.

3.4. Hardness field

Figure 6 shows the hardness field distribution during the heat treatment process. **Figure 6(a)** represents the hardness distribution after quenching heating. Since austenite has a lower hardness than pearlite, the hardness of the austenitized area is approximately 20 HRC, while

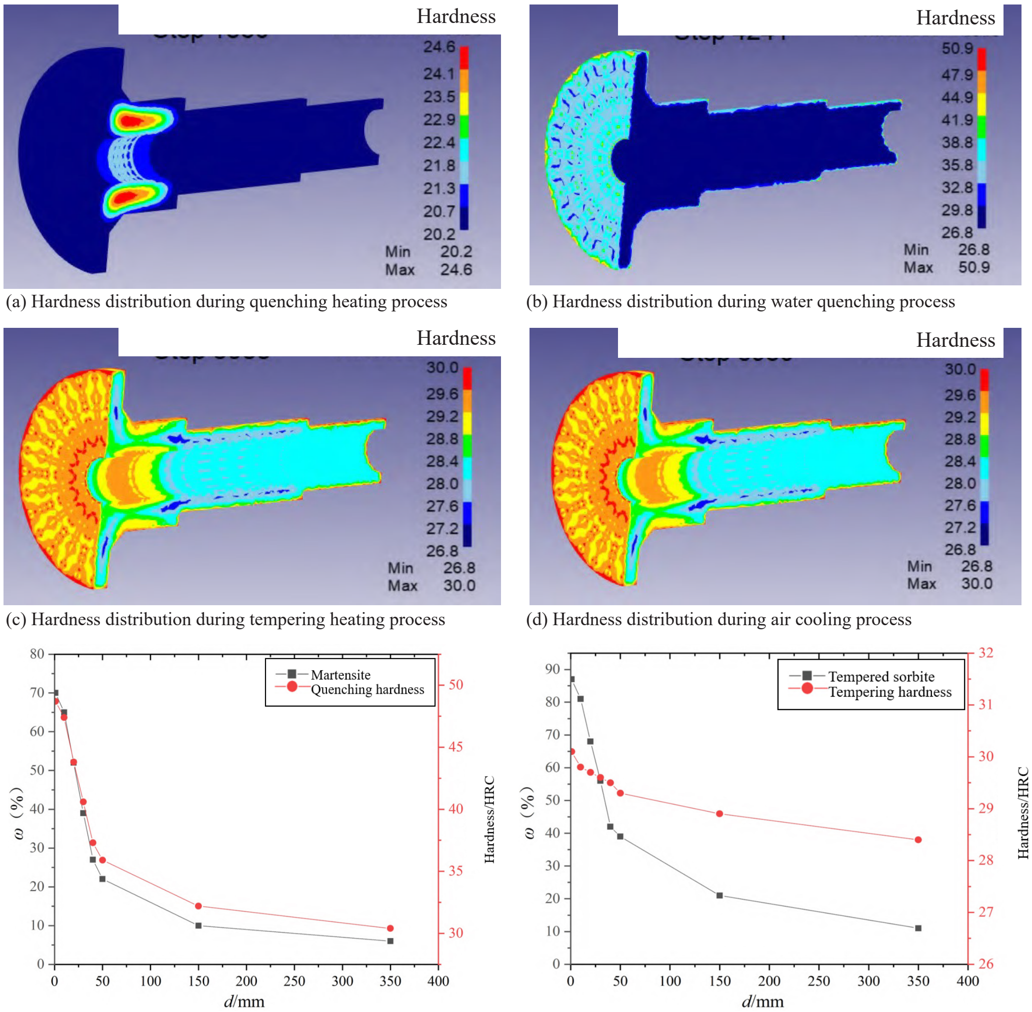

(a) Hardness distribution during quenching heating process
(b) Hardness distribution during water quenching process
(c) Hardness distribution during tempering heating process
(d) Hardness distribution during air cooling process
(e) Curve of martensite and hardness variation with distance during water quenching process
(f) Curve of tempered sorbite and hardness variation with distance during tempering process

Figure 6. Changes in hardness field during heat treatment of the fan's main shaft

the hardness of the pearlite area ranges between 23–25 HRC. After water quenching, the hardness of the main shaft increases significantly (**Figure 6(b)**). The formation of martensite increases the surface hardness of the main shaft to above 40 HRC, while the core has a lower martensite content and a hardness of only 27 HRC, which is slightly higher than the core hardness after quenching heating. Rapid cooling can make the grains finer, resulting in increased hardness. After tempering heating, due to the transformation of martensite into tempered sorbite, the stress decreases, and the hardness also decreases (**Figure 6(c)**). The maximum hardness is 30 HRC, indicating a stable phase with a relatively uniform hardness distribution. After air cooling, there is minimal change in hardness, and the hardness field remains stable with a uniform hardness distribution (**Figure 6(d)**). To study the variation trend of phase structure and hardness with distance during water quenching and tempering heating processes, a point tracking experiment was conducted at the end flange position (the flange is the most critical part of the wind turbine main shaft). Eight points were taken sequentially from the top surface of the flange, with an interval of 10 mm between each point (except for the 7th point with a 100 mm interval and the 8th point with a 200 mm interval). The results were plotted as curves showing the variation of water-quenched phase composition and hardness with distance (**Figure 6(e)**), as well as the variation of tempered phase composition and hardness with distance (**Figure 6(f)**). During the quenching process, as the distance from the surface increases, both

Table 4. Results of computer-simulated heat treatment process

Scheduling	Ending steps	Average temperature/°C	Average stress/MPa	Phase composition and proportion	Average hardness/ HRC
Quenching heating	1560	813.5	7.8	90%A+10%P(B)	20.9
Water cooling	4241	25.0	67.7	80%P(B)+10%M+10%F	30.0
Tempering heating	5935	594.9	27.4	80%P+10%Tempering S+10%F	28.6
Air cooling	6980	25.3	36.5	80%P+10%Tempering S+10%F	28.6

Table 5. Actual heat treatment experiment results [6]

Position	Phase composition	Hardness/HRC
12.5 mm below the surface	Tempered sorbite + bainite + a small amount of ferrite	27.5 ~ 30.0
1/3R position	Tempered sorbite + bainite + pearlite + ferrite	23.0 ~ 27.5

the martensite content and hardness decrease significantly. At a distance of 50 mm from the surface, the martensite proportion drops to about 20%, and the hardness is below 30 HRC. This suggests that martensite is mainly distributed within a 50 mm range from the surface of the flange. During the tempering process, the tempered sorbite content also decreases with increasing distance from the surface, following a similar trend as martensite. This indicates that tempered sorbite is primarily formed from the transformation of martensite. Since pearlite and tempered sorbite have similar hardness values, there is minimal variation in tempering hardness with distance.

The summary of the analysis results from the computer-simulated heat treatment is presented in **Table 4**. When compared to experimental data from published articles, as shown in **Table 5**, it is found that the phase composition and hardness range are generally consistent with the experimental data [6]. This suggests that computer simulation technology can be used to assist production practices, thereby improving production efficiency and reducing trial-and-error costs, providing theoretical support for the development of heat treatment processes. To further enhance the accuracy of finite element simulations, subsequent comparisons with experimental results and continuous calibrations are necessary.

4. Conclusion

Using computer simulation technology to simulate the heat treatment process of 42CrMo4 alloy steel wind turbine main shafts, the following conclusions are drawn: (1) A quenching temperature 70°C higher than the austenite-ferrite phase transformation temperature can achieve over 90% austenitization of the main shaft. To achieve a higher degree of austenitization, the temperature needs to be further increased, but excessively high temperatures can lead to coarse grains in the main shaft, reducing its strength and ductility. (2) Water quenching can generate significant stress within the main shaft, with a maximum of 354 MPa, posing a risk of cracking. Tempering can effectively reduce the internal stress of the main shaft, with the maximum stress decreasing to 119 MPa, a reduction of 66%. After air cooling, the maximum stress increases to 148 MPa. Appropriate stress can contribute to strain hardening phenomena, improving the overall mechanical properties of the main shaft. (3) After water quenching, the main shaft obtains approximately 10% martensite, mainly distributed within 50 mm of the surface. Through high-temperature tempering, it can be transformed into tempered sorbite. The final microstructure consists of pearlite, bainite, tempered sorbite, and ferrite, which is generally consistent with experimental data from the literature. (4) The increase in hardness of the main shaft is directly proportional to the martensite content. As the distance from the surface increases, both the martensite content and hardness decrease significantly, following the same trend. At a distance of 50 mm from the surface, the martensite proportion drops to about 20%, and the hardness is below 30 HRC. There is little difference in hardness between tempered sorbite and pearlite, and the final hardness range of the main shaft is approximately 27–30 HRC, which aligns with experimental data from the literature.

(5) Computer simulation technology can be applied to predict the heat treatment results of large castings and forgings. Combined with production practice data, it can further improve accuracy and provide theoretical support for developing heat treatment processes.

Funding

National Natural Science Foundation of China (51401113); Natural Science Foundation of Heilongjiang Province (E2016069); Key Research and Development Program of Heilongjiang Province (GZ20210034); Open Project of Key Laboratory of Polymer Matrix Composites in Heilongjiang Province (CLKFKT2021B7); Innovation and Entrepreneurship Training Program for College Students of Qiqihar University (202110232214)

Disclosure statement

The authors declare no conflict of interest.

References

[1] Shen X, 2016, Numerical Simulation and Applied Research on the Quenching Process of Wind Turbine Main Shaft, dissertation, Chongqing University.

[2] Chang C, Hu Y, 2021, Optimization of Heat Treatment Process for Forged Wind Turbine Main Shaft. Large Castings and Forgings, 2021(03): 43–44.

[3] Sui J, 2019, Finite Element Simulation of Quenching Process for Large Wind Turbine Main Shaft, dissertation, Shandong University.

[4] Yang K, Shi L, Cheng L, et al., 2018, Effect of Quenching and Cooling Process on Microstructure and Mechanical Properties of 42CrMo4 Wind Turbine Main Shaft. Metalworking (Thermal Processing), 2018(06): 93–95.

[5] Sakkaki M, Sadegh Moghanlou F, Parvizi S, et al., 2020, Phase Change Materials as Quenching Media for Heat Treatment of 42CrMo4 Steels. Journal of Central South University, 27(3): 752–761.

[6] Lu Y, Wang K, Liang X, et al., 2020, Optimization of Quenching and Tempering Process for 42CrMo4 Wind Turbine Main Shaft. Heat Treatment Technology and Equipment, 41(05): 29–32.

[7] Simsir C, Gur CH, 2008, A FEM-based Framework for Simulation of Thermal Treatments: Application to Steel Quenching. Computational Materials Science, 44(2): 588–600.

[8] Zhang X, Tang JY, Zhang XR, 2017, An Optimized Hardness Model for Carburizing-Quenching of Low Carbon Alloy Steel. Journal of Central South University, 24(1): 9–16.

[9] Sugianto A, Narazaki M, Kogawara M, et al., 2009, Distortion Analysis of Axial Contraction of Carburized-Quenched Helical Gear. Journal of Materials Engineering and Performance, 19(2): 194–206.

[10] Chaouch D, Guessasma S, Sadok A, 2012, Finite Element Simulation Coupled to Optimization Stochastic Process to Assess the Effect of Heat Treatment on the Mechanical Properties of 42CrMo4 Steel. Materials & Design, 34: 679–684.

[11] Sugianto A, Narazaki M, Kogawara M, et al., 2009, A Comparative Study on Determination Method of Heat Transfer Coefficient Using Inverse Heat Transfer and Iterative Modification. Journal of Materials Processing Technology, 209(10): 4627–4632.

[12] Xu Y, Huang G, 2013, Handbook of Heat Treatment Volume 1, 4th Edition, China Machine Press, Beijing.

[13] Shi K, Guo F, An L, et al., 2021, Heat Treatment Process of 42CrMo4 Steel for Wind Turbine Main Shaft. Metal Heat Treatment, 46(08): 201–204.